International Journal of Pharmaceutics 608 (2021) 121116

Contents lists available at ScienceDirect

International Journal of Pharmaceutics

journal homepage: www.elsevier.com/locate/ijpharm

Towards a better mechanistic comprehension of drug permeation and absorption: Introducing the diffusion-partitioning interplay

Martina M. Tzanova [a], Elizabeta Randelov [a], Paul C. Stein [b], Marianne Hiorth [a], Massimiliano Pio di Cagno [a,*]

[a] Department of Pharmacy, Faculty of Mathematics and Natural Sciences, University of Oslo, Norway
[b] Department of Physics, Chemistry and Pharmacy, University of Southern Denmark, Odense, Denmark

ARTICLE INFO

Keywords:
Unstirred water layer
UV–visible localized spectroscopy
Permeability
Permeapad®
Dynamic viscosity
Poly(ethylene glycol) (PEG)

ABSTRACT

The process of passive drug absorption from the gastrointestinal tract is still poorly understood and modelled. Additionally, the rapidly evolving field of pharmaceutics demands efficient, affordable and reliable *in vitro* tools for predicting *in vivo* performance. In this work, we combined established methods for quantifying drug diffusivity (localized UV-spectroscopy) and permeability (Permeapad® plate) in order to gain a better understanding of the role of unstirred water layers (UWLs) in drug absorption. The effect of diffusion/permeability media composition and viscosity on the apparent permeation resistance (R_{app}) of model drugs caffeine (CAF) and hydrocortisone (HC) were tested and evaluated by varying the type and concentration of viscosity-enhancing agent – glycerol or a poly(ethylene glycol) (PEG) with different average molecular weights. For all types of media, increased viscosity lead to reduction in diffusivity but could not alone explain the observed effect, which was attributed to intermolecular polymer-drug interactions. Additionally, for both drugs, smaller hydrophilic viscosity-enhancing agents (glycerol and PEG 400) had larger influence than larger ones (PEG 3350 and 6000). The results highlighted the role of UWL as an additive barrier to permeation and indicated that diffusion through UWL is the rate-limiting step to CAF's permeation, whilst HC permeability is a partition-driven process.

1. Introduction

Oral delivery remains the major route of drug administration (Zhong et al., 2018) for numerous reasons, such as high patient compliance and ease of administration. The rate and extent of drug absorption largely define drug bioavailability and, consequently, the therapeutic outcome. In this context, the prediction of drug bioavailability and *in vivo* formulation performances through *in vitro* methods has become highly desirable. Independently of the type of formulation, once administered orally, it needs to release the active pharmaceutical ingredient (API), which then needs to be absorbed through the gastrointestinal (GI) wall and into the blood stream before it can reach its designated site of action. In general, drug absorption takes place largely through passive diffusion through a barrier composed of: a mucus layer (a stagnant polymeric/aqueous layer that lies on the apical side of enterocytes) and an enterocyte cellular layer.

In the last three decades, research has been focused on better understanding and modelling the mechanism of permeation through cells and biomimetic barriers, leaving the unstirred layers (such as mucus) behind. Several *in vitro* permeability assays have been developed and are largely employed in pharmaceutical research and development – both cell-based (Artursson et al., 1991; Kwatra et al., 2011) and cell-free (Berben et al., 2018). One of the latest *in vitro* cell-free permeation assays is Permeapad® (Di Cagno et al., 2015). Permeapad® is also available in 96-well-plate ready-to-use format, allowing high-throughput screening of new chemical entities (NCEs) and novel formulations in a rapid and reliable manner. All *in vitro* permeability methods have similarities in their set-up, as they are based on a two-compartment system, consisting of a donor drug solution (or dispersion), an acceptor solution and a barrier separating the two compartments. The underlying assumption for data interpretation (i.e. measuring of an apparent permeability coefficient, P_{app}) of all these methods are that:

1. Drug diffusion takes place in a one-phase system (i.e. No physical interfaces present), allowing the utilization of Fick's law of diffusion (Eq. (1)) for describing the diffusion process:

* Corresponding author at: Department of Pharmacy Faculty of Mathematics and Natural Sciences, P.O.Box 1068, Blindern 0316 Oslo, Norway.
E-mail address: m.p.d.cagno@farmasi.uio.no (M.P. di Cagno).

https://doi.org/10.1016/j.ijpharm.2021.121116
Received 16 June 2021; Received in revised form 13 September 2021; Accepted 16 September 2021
Available online 20 September 2021
0378-5173/© 2021 The Author(s). Published by Elsevier B.V. This is an open access article under the CC BY license (http://creativecommons.org/licenses/by/4.0/).

$$j = -D\frac{dc}{dx} \quad (1)$$

where, j represents the net flux of the drug through the barrier (μmol/cm^2·s), D – the diffusion constant (cm^2/s) and dc/dx – the concentration gradient.

2. The permeation barrier is homogeneous and a constant concentration gradient between donor and acceptor solutions exists.

Thus, *in vitro* permeability assays can be said to measure "bulk" permeability. As depicted in Fig. 1, a drug concentration gradient exists within each of these layers and the conventional methods for determining P_{app} do not discriminate between the roles played by each of the layers on drug permeation. In reality, unstirred water layers (UWLs) exist at each membrane-solution interface and may act as an additional permeation barrier. Even though the importance of the UWL in permeation studies has been highlighted (Avdeef et al., 2001, Brewster et al., 2007, Korjamo et al., 2009) and standard mathematical models, describing mass transport in membrane permeation, take it into account (Barrie et al., 1963; Flynn et al., 1974; Grassi and Colombo, 1999), the role that this "additive" layer plays in the permeation processes remain still largely unknown and understudied. Our belief is that neglecting the role of UWL in permeation makes the achievement of reliable *in vitro/in vivo* correlation not possible. Additionally, the presence of a mucus UWL *in vivo* in the human intestine is evident but due to the high intestinal mobility has a significantly lower thickness than *in vitro* UWLs – 30–100 μm *in vivo* (Lennernäs, 1998) versus 500–1200 μm for *in vitro* cell-based and as much as 4000 μm for some cell-free assays (Avdeef et al., 2004).

An alternative way to describe the permeation process through a barrier composed of consecutive layers is to utilize the *resistivity*. Per definition, a chemical entity's apparent resistance to permeation (R_{app}) is the inverse of its apparent permeability (P_{app}; Eq. (2)). Similar to electrical resistors, the resistance generated by each permeated layer can be added together to calculate to total resistance of the permeation barrier (Loftsson et al., 2006):

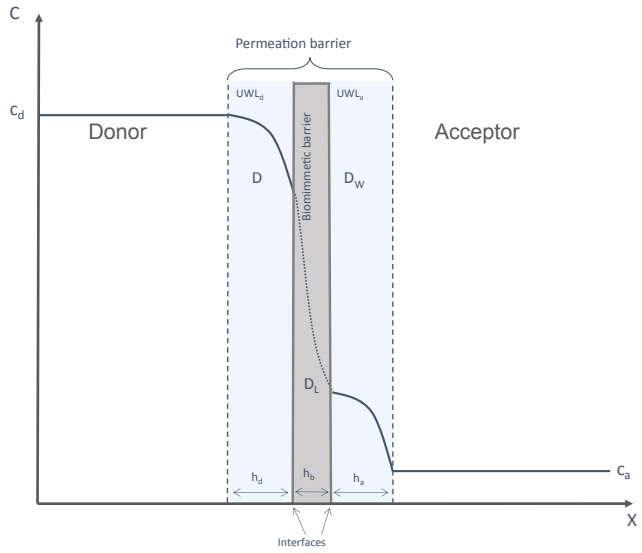

Fig. 1. Concentration gradients in a generalized two-compartment permeability system with unstirred water layers (UWLs) on each side of a biomimetic barrier, constituting the complete permeation barrier. D, D_W and D_L represent the diffusion coefficients in the donor medium, water and lipid, respectively; h_d, h_a and h_b – the thickness of UWL in the donor and acceptor compartment, and the biomimetic barrier, respectively, whereas c_d and c_a are the drug concentrations in the donor and acceptor compartments, respectively.

$$P_{app} = \frac{1}{R_{app}} = (R_d + R_{eff} + R_a)^{-1} = \left(\frac{1}{P_d} + \frac{1}{P_{eff}} + \frac{1}{P_a}\right)^{-1} \quad (2)$$

where, R_d, R_{eff} and R_a are the resistivity of the UWL in the donor compartment, the effective resistivity (through the biomimetic barrier itself) and the resistivity of the UWL in the acceptor compartment, respectively.

The aim of the present study was to clarify the role of the UWLs in the permeation process. For this purpose, we measured the diffusivity constants of model drugs caffeine (CAF) and hydrocortisone (HC) in a stagnant media using localized UV–Vis spectroscopy. The method involves the collection of numerous data points at a specific location within the sample cuvette, which describe the change in *local* drug concentration and ultimately constitute the drug diffusion profile (Di Cagno et al., 2018). Subsequently, we combined this information with permeability data obtained by an *in vitro* permeability assay (Permeapad®). In order to alter the UWL characteristics (composition and viscosity), the neutral hydrophilic polymer poly(ethylene glycol) (PEG) of different molecular sizes and at different concentrations were added in the donor compartment. For comparison, a low-molecular-weight hydrophilic moiety, glycerol, was also examined in an array of concentrations.

2. Materials and methods

2.1. Materials

Caffeine (CAF), hydrocortisone (HC), 1-octanol (for HPLC, ≥ 99%) and sodium hydroxide (≥98.0% pellets; NaOH) were purchased from Sigma-Aldrich Chemie GmbH (Steinheim, DE). Acetonitrile (≥99.9% isocratic grade for HPLC; ACN), sodium chloride (NaCl) and sodium dihydrogen phosphate dihydrate ($NaH_2PO_4{\cdot}2H_2O$) were purchased from VWR Chemicals (Radnor, PA, USA). Disodium phosphate dihydrate ($Na_2HPO_4{\cdot}2H_2O$), glycerol for analysis, poly(ethylene glycol) 400 for synthesis (PEG 400) and poly(ethylene glycol) 6000 for synthesis (PEG 6000) were purchased from Merck KGaA (Darmstadt, DE). Kollisolv® PEG 3350 USP LAX was a generous gift from BASF Corporation (Florham Park, NJ, USA). All solutions were prepared with water, purified by a Milli-Q® water purification system for ultrapure water by Merck Millipore (Darmstadt, DE).

2.2. Preparation of solutions

Phosphate-buffered saline (PBS) 73 mM pH 7.4 was prepared by mixing one part 2.5% (w/v) $NaH_2PO_4{\cdot}2H_2O$ solution with four parts 0.9% (w/v) $Na_2HPO_4{\cdot}2H_2O$ solution. The pH was subsequently adjusted to 7.4 ± 0.05 (SevenCompact™ pH/ion meter S220; Mettler Toledo, Columbus, OH, USA) by the addition of NaOH pellets and osmolality – to 280–300 mOsm/kg (Semi-Micro Osmometer K-7400, Knauer, Berlin, DE) by the addition of NaCl. PBS was filtered 0.2 μm (Whatman® Nuclepore Track-Etch membrane filter; GE Healthcare Life Sciences, Maidstone, UK) prior to use.

Mixtures of water or PBS and a viscosity-enhancing agent (glycerol, PEG 400, PEG 3350 or PEG 6000) were prepared in a variety of concentrations (w/v percentage; denoted: %).

2.3. Viscosity

The dynamic viscosity (mPa·s) of mixtures of water and glycerol (5, 10, 25, 50 and 60%), PEG 400 (2.5, 5, 10, 25 and 40%), PEG 3350 (1, 2.5, 5, 10, 15 and 25%) or PEG 6000 (1, 5, 10, and 15%) was measured on Physica MCR 301 rheometer with cone-plate geometry (cone: CP75-1; Anton Paar, Graz, AU). Samples (2.4 mL; n = 3) were applied to the instrument plate, trimmed in a reproducible manner and allowed to rest/equilibrate for 5 min. Rotational measurements were performed at

25 ± 0.1 ℃ over an appropriate range of shear rates (100 – 2000 s^{-1}), depending on the sample. Only values from the infinite-shear viscosity plateau were used further to calculate the average dynamic viscosity of all measurement points for a given sample. Measured viscosity values of the different solutions employed allowed the correlations between diffusivity and permeability for different compounds tested.

2.4. Diffusivity

2.4.1. Experimental procedure

Drug diffusion was quantified using the localized spectroscopy method originally described by Di Cagno et al. (2018). Measurements were performed on a double array UV–Vis spectrophotometer UV-6300PC (VWR International, Radnor, PA, USA) in semi-micro cuvettes with PTFE stopper ($V_{chamber}$ = 700 μL, path length = 10 mm; Starna Scientific®, Essex, UK). The diffusion media and reference sample (675 μL each) consisted of one of the following – water, glycerol (5, 25 and 60%), PEG 400 (2.5, 5, 10, 25 and 40%), PEG 3350 (2.5, 10, and 25%) or PEG 6000 (1, 5, 10, 15 and 25%). The donor solution contained CAF (1 mM) or HC (0.5 mM), dissolved in pure PBS or, alternatively, in buffered solution of the appropriate viscosity-enhancing agent. At time zero (t = 0 s), donor solution (25 μL) was injected at the bottom of the sample cuvette using a microneedle syringe (Hamilton Company, Reno, NV, USA). Absorbance measurements were recorded at 273 and 248 nm for CAF and HC, respectively, every 120 s for a total of 21 – 27 h (longer measurements for the more viscous samples). For all experiments, the sample cuvette was lifted by precisely 0.60 cm using a 3D-printed stand, in order to record absorbances at precisely 0.51 cm from the bottom of the cuvette (i.e. the origin of diffusion, (Di Cagno et al. 2018)). Three independent experiments (n = 3) were performed for each drug in the following diffusion media – water, 60% glycerol, 40% PEG 400, 25% PEG 3350 or 15% PEG 6000.

2.4.2. Data analysis

Diffusion coefficients were calculated using the mathematical approach previously described by Di Cagno et al. (2018). The diffusion equation (Fick's second law of diffusion; Eq. (3)) describes the spontaneous migration of molecules in a homogeneous medium as:

$$\frac{\partial c(x,t)}{\partial t} = D\frac{\partial^2 c(x,t)}{\partial x^2} \tag{3}$$

where, c is the concentration of diffusing species, x is the position (cm), t is the time (s) and D is the diffusion coefficient (cm^2/s). An analytical solution of Eq. (3) can be compiled (Di Cagno et al., 2018):

$$c(x,t) = \frac{A}{\sqrt{\pi}}\frac{e^{\frac{-x^2}{2\sigma^2+4Dt}}}{\sqrt{2\sigma^2+4Dt}} \tag{4}$$

where A, D and σ are fitting parameters corresponding to the initial amount of API in the donor solution ($mmol/cm^2$), the diffusion coefficient and the width of the initial drug distribution (cm; assuming a half Gaussian initial distribution), respectively. The derivation of Eq. (4) is only possible under the following assumptions:

1. That the observation point, x, is closed to the source than the end of the tube, i.e. × is such that × ≪ h
2. That the diffusing particles cannot reach the end of the tube by the end of the experiment, i.e. t is such that $t \ll h^2/D$

Experimental data (obtained as described in later section 2.4.1), was fitted to Eq. (4) in order to extract diffusion coefficients. The excellent goodness of fit (R^2) of the model to the experimental data both in this study (see Table S2) and earlier studies (e.g. Di Cagno et al., 2018; Di Cagno and Stein, 2019; Falavigna et al., 2020) confirms the validity of the above assumptions.

2.5. Permeability

2.5.1. Experimental procedure – Permeapad® plate

CAF and HC permeability though an artificial biomimetic barrier was investigated using the high-throughput 96-well Permeapad® plate (InnoMe GmbH, Espelkamp, DE). PBS pH 7.4 was used as acceptor solution (400 μL). The donor (200 μL) consisted of an API solution in either plain PBS, 60% GLY-PBS, 40% PEG 400-PBS, 25% PEG 3350-PBS or 15% PEG 6000-PBS (Table 1). After filling both acceptor and donor compartments, the plate was sealed with Parafilm® (Sigma-Aldrich, Saint Louis, MO, USA) to reduce evaporation and incubated in an orbital shaker-incubator (ES-20, Biosan, Riga, LV) at 25 ℃ and 200 rpm for a total of 4 h. Samples (120 μL) were taken from the acceptor every 30 min and the withdrawn volume was replaced with fresh PBS. Experiments were repeated in triplicate (n = 3).

2.5.2. Quantification methods

Samples containing CAF were directly transferred upon withdrawal to a UV-transparent 96-well microliter plate (Corning Inc., Kennebunk, ME, USA) and absorbance was measured at 273 nm on a microplate spectrophotometer (SpectraMax 190, Molecular Devices Inc., Sunnyvale, CA, USA). Standard solutions (concentration range: 5 – 100 μM; $R^2 \geq 0.9999$) were measured on the same plate and blank absorption (PBS) was deducted from all measurements.

Samples containing HC were analysed using high-performance liquid chromatography with ultraviolet detection (HPLC-UV) at 254 nm. The analysis was performed on an UltiMate 3000RS system (Thermo Scientific™ Dionex™, Sunnyvale, CA, USA), equipped with a Nova-Pak C18 guard column (3.9 × 20 mm) and column (3.9 × 150 mm, 60 Å, 4 μm; Waters™, Milford, MA, USA). Isocratic elution was utilized with mobile phase, consisting of ACN:water (35:65; on-line mixing) and a flow rate of 1 mL/min. Column oven temperature was set at 30 ℃, the retention time was 2.4 min and the total run time was 5 min. The injection volume was 40 μL and two injections per vial were analysed. Standard solutions (concentration range: 0.05 – 100 μM; $R^2 \geq 0.99999$) were analysed in a similar manner in the beginning, middle and the end of each sequence, to ensure system changes were detected and could be accounted for.

2.5.3. Data analysis

The cumulative amount of drug permeated though the barrier (Q; μmol), divided by the membrane surface area (SA = 0.13 cm^2; diameter = 5 mm) was plotted as a function of time (t; s) and the flux (j; μmol/cm^2·s) was calculated from the slope of the linear regression obtained in the steady-state region (Eq. (5)).

$$j = \frac{1}{SA} \times \frac{dQ}{dt} \tag{5}$$

In order to obtain the apparent permeability coefficient (P_{app}, cm/s) fluxes were normalized by the initial donor concentration of the drug (c_0; mM) as shown in Eq. (6):

$$P_{app} = \frac{j}{c_0} \tag{6}$$

Further, combining Eqs. (2) and (6) with the assumption that the

Table 1
General characteristics (M_w, molecular weight; pKa, acid dissociation constant; λ_{max}, wavelength of maximum absorbance in PBS pH 7.4; and ε, molar extinction coefficient) and concentrations of donor solutions for permeability and diffusion experiments (c_d) of the investigated compounds (*API*).

API	M_w g/mol	pKa[a]	λ_{max} nm	E cm^2/mol	c_d mM
Caffeine (CAF)	194.2	14	273	10.05	1 *or* 2[b]
Hydrocortisone (HC)	362.5	–	248	15.04	0.5

[a] Source: Sigma-Aldrich. *Caffeine (anhydrous): Product information.*
[b] Diffusion – 1 mM solution, permeability – 2 mM solution.

UWLs of the acceptor and the donor compartments have the same thickness ($h_d = h_a$) (since the plates were stirred by an orbital shaker) and considering that the resistivity through the UWL can be calculated from the measured drug diffusivities in the two different compartments, Eq. (7) is obtained.

$$R_{app} = \frac{h_d}{D} + R_{eff} + \frac{h_a}{D_w} \quad (7)$$

where, D and D_w are drug diffusivity values in the donor and acceptor media, respectively. Arbitrary, in this work, the thickness of the UWL ($h_d = h_a$) was assumed to be 800 μm in both compartments (Karlsson and Artursson 1991; Avdeef et al., 2004; Korjamo et al., 2009).

2.6. Distribution coefficient

CAF and HC were dissolved in each of the following solvents: PBS, 60% GLY-PBS, 40% PEG 400-PBS, 25% PEG 3350-PBS and 15% PEG 6000 in a concentration of 2 mM and 0.5 mM, respectively. Equal volumes of each API solution and 1-octanol were mixed in a glass vial and allowed to stand for a minimum of 72 h. Additionally, octanol-saturated solvents were obtained by mixing each solvent with octanol by the same procedure. The aqueous phase of each sample was carefully extracted, diluted with the appropriate octanol-saturated solvent and the drug concentration was quantified by UV–Vis spectrophotometry (octanol-saturated solvent used as a blank). Calibration curves for each drug were prepared in octanol-saturated PBS. Finally, distribution coefficient ($K_{o/w}$) values were calculated by Eq. (8), where c_o and c_w are the drug concentrations (mM) in the octanol and aqueous phase, respectively.

$$K_{o/w} = \frac{c_o}{c_w} \quad (8)$$

3. Results and discussion

3.1. Viscosity

In order to evaluate the effect of media viscosity on the passive diffusion and permeability of model drugs CAF and HC, the dynamic viscosity of glycerol and PEG mixtures with water at different concentrations was determined. Measurement points at varying shear rates within the infinite-shear viscosity plateau were used to calculate a mean value, representative of the viscosity of the solution (i.e. η_∞). Further, the effects of different solvent (water vs PBS) and the presence of drug were evaluated (results not presented). Both factors were found to have a negligible effect on the measured viscosity (<1% deviation, i.e. within the limits of experimental error). Measurements were therefore performed in the absence of drug on mixtures of glycerol/PEG and water.

The results (Fig. 2) showed an expected (Hou et al., 2011; Bhanot et al., 2012) exponential relationship between the glycerol/PEG concentration and the dynamic viscosity. A strong correlation ($R^2 > 0.99$) was observed for all series when the data was fitted to Eq. (9):

$$\eta = \eta_w e^{\lambda c} \quad (9)$$

where, η and η_w are the dynamic viscosity values of any given mixture and of water, respectively, c is the concentration of viscosity-enhancing agent and λ is a fitting parameter. For the homologous series of PEG species examines, λ could be correlated linearly ($R^2 = 0.999$) with the molecular weight (M_w) of the polymer by Eq. (10), where a_1 and b_1 are fitting parameters (for values: Supplementary material, Table S1):

$$\lambda = a_1 M_w + b_1 \quad (10)$$

Generally, the results showed the slowest concentration-dependant viscosity increase for the glycerol mixtures, a steeper increase was observed for the PEGs and the larger species (i.e. larger average M_w) showed a much steeper increase in viscosity at comparable concentrations.

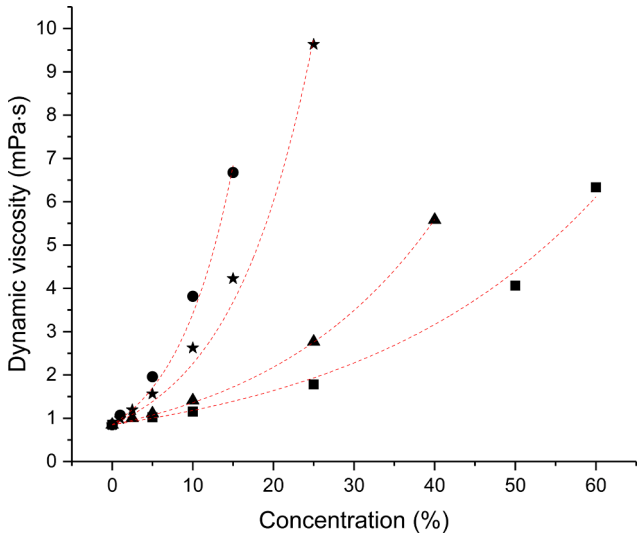

Fig. 2. Dynamic viscosity of aqueous solutions of (left to right) PEG6000 (●), PEG3350 (★), PEG400 (▲) and glycerol (■) as a function of concentration. Red dashed lines show curves fitted to the data according to Eq. (9) (fitting parameters summarized in Supplementary material, Table S1). RSD ≤ 4% (n = 3) for all values.

3.2. Diffusion

3.2.1. Diffusion and concentration

The relationships and correlation between the measured parameters were examined using graphical plotting and data fitting on the data analysis software Origin® (OriginLab Corporation, Northampton, MA, USA). For all data fits, goodness of fit was evaluated and data are presented as a Supplementary material.

Passive drug diffusion of CAF and HC in plain water (D_w) and mixtures of water and one of several viscosity-enhancing agents (D) was investigated with a localized spectroscopic method, as described earlier (Di Cagno et al. 2018). D_w for CAF and HC were measured to be 7.18 and 4.84 × 10^{-6} cm^2/s, respectively. These results are slightly lower than previous findings using the same method (Di Cagno et al. 2018 and 2019, Falavigna et al. 2020) and in good agreement with values measured with different approaches (Price 1989, Blokhina et al. 2017). The reproducibility of the measurements was evaluated by looking at the relative standard deviations (RSD) of three independent replicates of D_w and D for the highest concentrations of glycerol and each PEG. In water, glycerol, PEG 400, PEG 3350 and PEG 6000 for CAF, RSD was calculated to be 0.3, 11, 7, 6 and 2% and for HC 5, 3, 10, 8 and 4%, respectively. Such relatively low variation (≤11%), despite the dynamic and complex systems examined, implies credibility of the results and allows for reliable statistical inference based on them.

In Fig. 3 the variation in local concentration over time is exemplified with data for CAF diffusing through pure water (No PEG, black plot) and three different concentrations of PEG 400 in water: 10, 25 and 40% (blue, green and red plots, respectively). The figure illustrates the difference in the rate of drug diffusion with increasing polymer concentration and medium viscosity. The initial slope of each plot roughly describes the diffusivity of the drug in the given medium – the steeper the slope, the larger the diffusion coefficient. It is evident that increasing the polymer concentration has a large impact on drug diffusion through the media as the curves become progressively shallower, the higher the polymer concentration is. On the other hand, the highest concentration of the diffusion profiles is related to the initial drug concentration (A in Eq. (4)) and is the same for all experiments (Supplementary material, Table S2), in accordance with the identical nominal drug concentrations

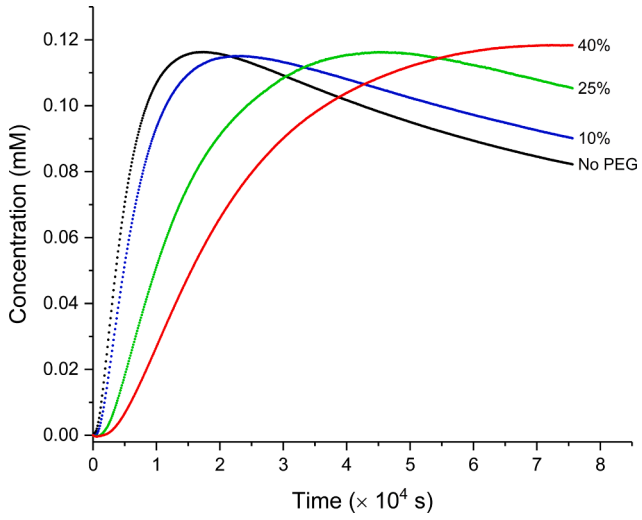

Fig. 3. Variation in local concentration measured at fixed distance from the origin of diffusion (x = 0.51 cm) for CAF in plain water (in black) and different concentrations of *PEG400*: 10% (in blue), 25% (in green) and 40% (in red) over time. After the initial 2 × 104 s, RSD ≤ 2% and 6% (n = 3) for *No PEG* and *40% PEG400*, respectively.

in the donor solutions.

The relationship between the diffusion coefficients and the concentration of viscosity-enhancing agent is depicted in Fig. 4. Interestingly, the reduction in diffusivity of both CAF and HC is described well ($R^2 \geq 0.89$) by the change in concentration of viscosity-enhancing agent, as shown in Eq. (11), where D and D_w are the drug diffusion coefficients in a given solution and in pure water, respectively, and μ is a fitting parameter:

$$D = D_w e^{-\mu c} \quad (11)$$

The fitting parameter, μ, describes the steepness/velocity of the exponential decay in diffusivity with increasing concentration of viscosity-enhancing agents (Fig. 5). This parameter can be used to approximate the effect of the UWL composition on the diffusivity of the tested drug. However, as it does not account for the viscosity, it might be insufficient to describe the entire phenomenon. For CAF, it appears that increased concentration of all hydrophilic polymers significantly reduces drug diffusivity but this effect is more pronounced for PEG 400 and PEG 6000 than for glycerol and PEG 3350 (i.e. larger μ). These findings are logical, as one would expect intermolecular interactions between CAF (hydrophilic substance, log $K_{o/w} < 1$) and a hydrophilic polymer in solution. Intriguingly, for HC, a sharper drop in diffusivity (i.e. larger μ) is observed when the drug diffuses through glycerol and PEG 400 in comparison to the larger PEGs. One possible explanation of the observed phenomenon could be the formation of a macromolecular complex of larger hydrodynamic radius between HC and glycerol/PEG400 (Hirai at al. 2018) and consequently reduced diffusivity. Moreover, the minor influence of larger hydrophilic polymers on the passive diffusion of HC in comparison to CAF is in agreement with the findings of Falavigna et al. (2020) that the passive diffusion of lipophilic drugs (e.g. HC) through an UWL is less affected by the presence of mucin

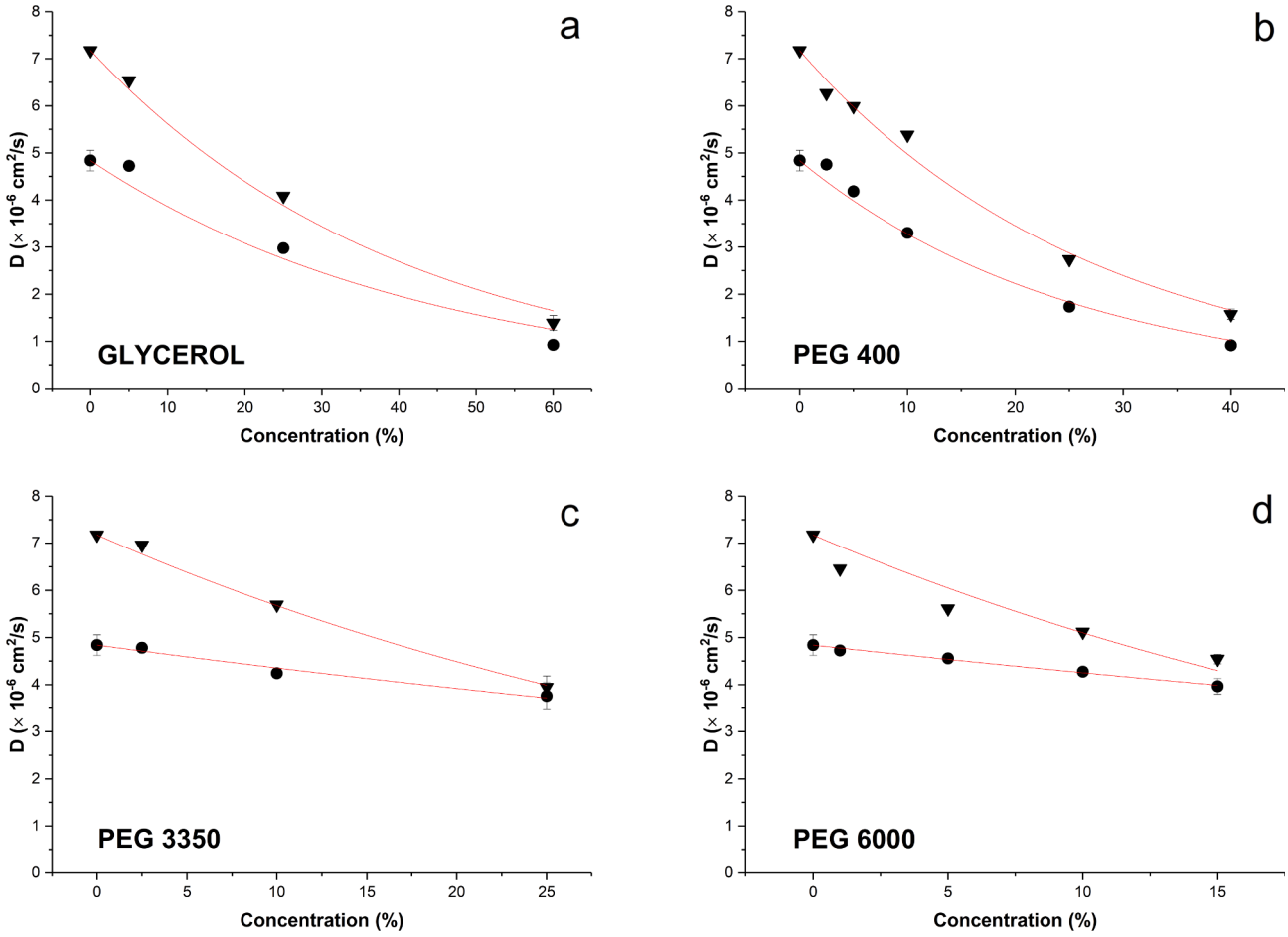

Fig. 4. Diffusivity (D) of CAF (▼) and HC (●) as a function of viscosity-enhancing agent concentration for: a) glycerol, b) PEG400, c) PEG3350 and d) PEG6000. Red lines show curves fitted to the data according to Eq. (11) (fitting parameters summarized in Supplementary material). Error bars show SD (n = 3).

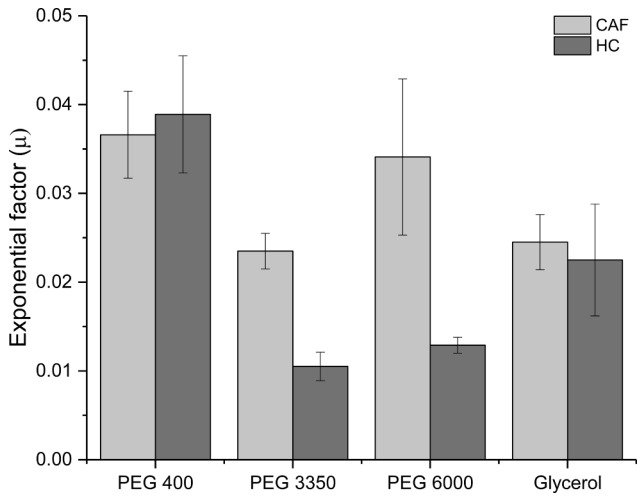

Fig. 5. Exponential factor (μ) corresponding to the best-fit parameter, as described by Eq. (11) and depicted in Fig. 4, illustrating the influence of the various hydrophilic moieties on CAF (light grey) and HC (dark grey). Error bars show SD (n = 4, 5 *or* 6, depending on number of data points).

in comparison to hydrophilic drugs (e.g. CAF). This phenomenon could be explained by the different ability of the two compounds in creating hydrogen bonds with the polymer. From these results, a generally higher resistance to permeation could be anticipated for both HC and CAF in the presence of a polymer in the solution.

3.2.2. *Diffusion and viscosity*

Further, the relationship between drug diffusivity in the various media and media viscosity was investigated (Fig. 6). From a theoretical point of view (Stokes-Einstein equation; Eq. (12)), drug diffusion in a homogeneous medium should solely depend on medium viscosity (η; mPa·s) and molecule size (hydrodynamic radius, r; cm), when the temperature (T; K) and k_B (Boltzmann constant; $cm^2 \cdot g/s^2 \cdot K$) are constant:

$$\frac{1}{D} = \left(\frac{6\pi}{k_B T}\right)\eta r \tag{12}$$

This suggests that the correlations represented in Fig. 6 (a – d) should be identical for a given API and that a direct linear correlation exists between media viscosity and the reciprocal diffusivity (1/D *or* D^{-1}; s/cm^2). Indeed, an adequate linear correlation ($R^2 \geq 0.85$, Eq. (13)) was observed between η and D^{-1}, with a slope a_2 and intercept – b_2 (where a_2 and b_2 are fitting parameters):

$$D^{-1} = a_2\eta + b_2 \tag{13}$$

However, this relationship deviates from Eq. (12) due to the coefficient $b_2 \neq 0$, confirming the presence of specific drug-polymer interactions, which have an effect on D beyond the viscosity of the diffusion media. This implies that Stokes-Einstein relation fails to explain the diffusivity of drugs in more complex matrices (e.g. in the presence of macromolecules such as polymers) and is a particularly important aspect to consider when studying drug diffusion through *in vivo* mucosal UWLs. To the best of our knowledge, this is the first time this has been demonstrated experimentally for drugs.

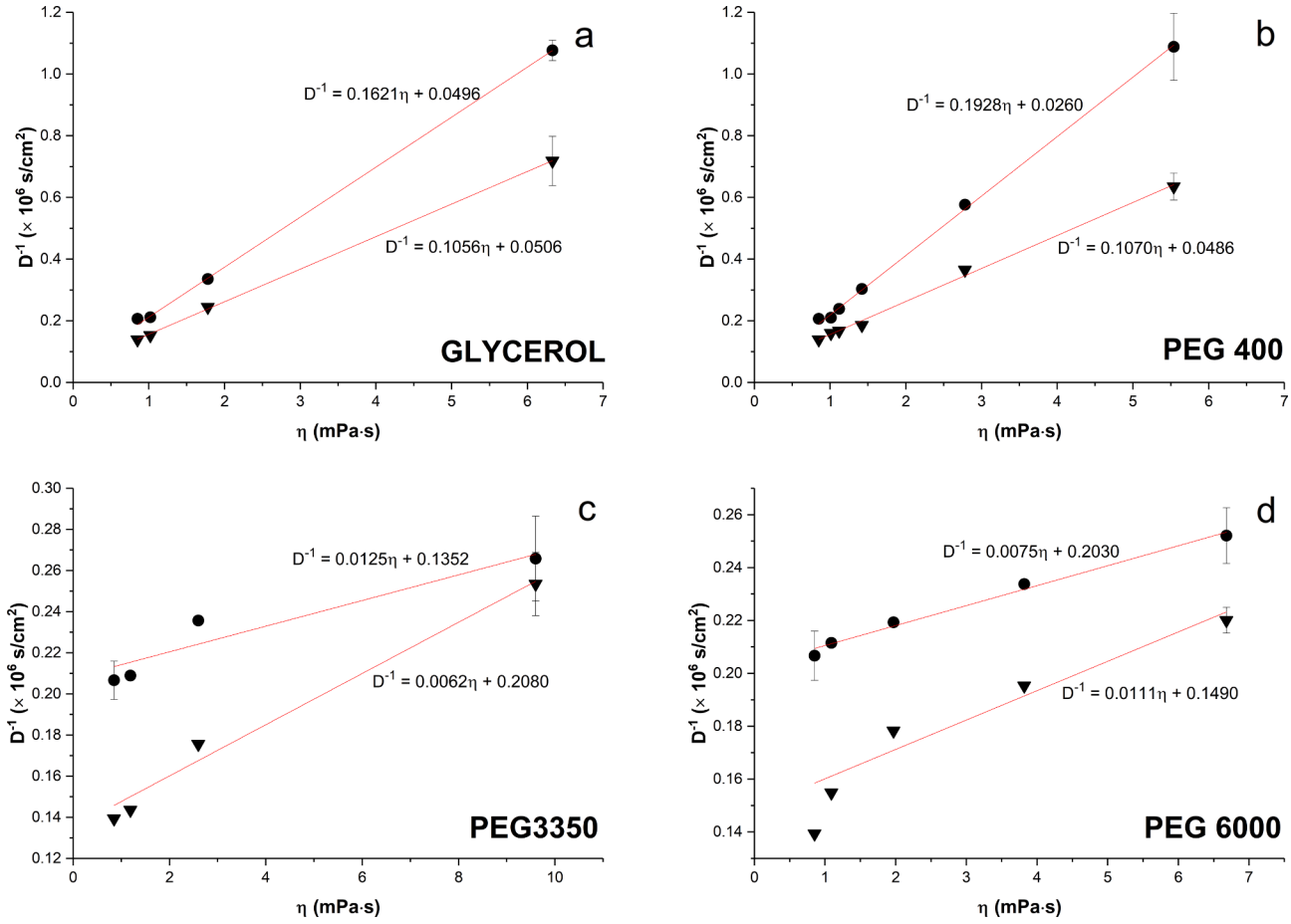

Fig. 6. Reciprocal diffusivity (D^{-1}) of CAF (▼) and HC (●) as a function of diffusion media viscosity (η) for: a) glycerol, b) PEG400, c) PEG3350 and d) PEG6000. Red lines show linear regression fitting to the experimental data according to Eq. (13) (fitting parameters summarized in Supplementary material). Error bars show SD (n = 3).

Further, as expected from its larger hydrodynamic radius in comparison to CAF, HC diffused slower than CAF in all media and at any given viscosity (Fig. 6). The viscosity-dependent diffusion of both APIs exhibited generally similar behaviour in glycerol and PEG 400, despite the chemical differences both between APIs and between viscosity-enhancing agents. This could be explained with the similar (in magnitude) molecular sizes of the two hydrophilic agents, which governs their ability to create a network and interact with the APIs. For both drugs, the results show a significant decrease in absolute diffusivity values and in the slope of the linear regressions (a_2) when comparing PEG 400 and glycerol profiles to the larger PEGs (3350 and 6000). However, for CAF there is a 10-fold reduction from the systems glycerol/PEG 400 to PEG 3350/PEG 6000, whereas, for HC, this drop is much larger – approximately 25-fold (Fig. 6). Thus, the results reveal a much stronger influence of glycerol and PEG 400 on the net diffusion of HC in comparison to CAF and a much larger influence of the UWL on the permeation process of HC in comparison to CAF could be anticipated.

A key aspect of our experimental approach was based on maintaining media viscosity, rather than the concentration of the viscosity-enhancing agent within the same range. Therefore, owing to the higher concentrations of glycerol and PEG 400, one explanation of the observed behaviour could be the formation of supramolecular complex between drug molecules and glycerol/PEG400 with a consequent enlargement of the hydration shell and of the hydrodynamic radius (r) of the drug. The molecular space of the two investigated drugs indeed plays a role in the magnitude of the observed phenomenon. For the larger PEGs, the highest concentrations (25 and 15%, respectively) appear to be outside the dilute solution region and the linear relationship proposed by Eq. (13) fails to describe this behaviour properly (hence lower R^2). This phenomenon could be attributed to differences between the measured bulk dynamic viscosity and the actual microviscosity, met by the drugs in the experimental setup. A good correlation between the two has been shown for smaller PEGs (Bhanot et al., 2012) but not for species of larger molecular weight. Furthermore, as shown in Fig. 6d, the diffusion coefficients seem to approach a plateau at high polymer concentration. In order to confirm this hypothesis, the diffusion of both APIs in a 25% PEG 6000 solution was measured. This diffusion medium had a viscosity of 28 mPa·s (extrapolated from the best-fit Eq. (9)) and the measured diffusivities were 3.98 and 3.78 $\times$ 10^{-6} (cm^2/s) for CAF and HC, respectively. For CAF this indicated approaching a plateau (D = (4.54 $\pm$ 0.10) $\times$ 10^{-6} cm^2/s for 15% PEG 6000) and confirmed the plateau for HC (D = (3.98 $\pm$ 0.17) $\times$ 10^{-6} cm^2/s for 15% PEG 6000). The difference between the two APIs can be explained with the difference in lipophilicity between the two drugs. For the hydrophilic CAF, the addition of more hydrophilic PEG leads to further reduction in diffusivity, whilst the diffusivity of HC reaches a plateau at much lower PEG concentrations as the further addition of a hydrophilic moiety leads to no further interactions between the polymer and the drug.

3.3. Permeability

Currently, several reliable methods for measuring apparent permeability coefficients (P_{app}) of APIs and NCEs are available, allowing the prediction of *in vivo* drug performance. One of the limitations of these methods is that the effect of UWL on the net permeation reprocess is disregarded. In this work, we utilized the diffusion constants measured in the different UWLs (as described earlier) in order to calculate drug resistances to permeation through each of the layers composing the barrier, namely R_u^d, R_{eff} and R_u^a (Eq. (7)). Giving the moderate stirring applied (200 rpm), and in accordance with available literature data for cellular (i.e. Caco-2) and non-cellular (i.e. PAMPA) permeability set-up (Karlsson and Artursson 1991; Avdeef et al., 2004) the UWL thickness was arbitrary assumed to be approximately 800 μm and to be of equal thickness in both donor and acceptor. The results showed in Fig. 7 evidence that CAF, in general, has a much – approximately tenfold – lower apparent resistance (R_{app}) than HC in all tested permeability media of comparable viscosity. A unique feature of Permeapad®, in comparison to other *in vitro* permeation tools (e.g. PAMPA), is that the liposomal gel-like structure composing the barriers can also account – to some extent – for paracellular permeation. Therefore, the higher permeability of CAF

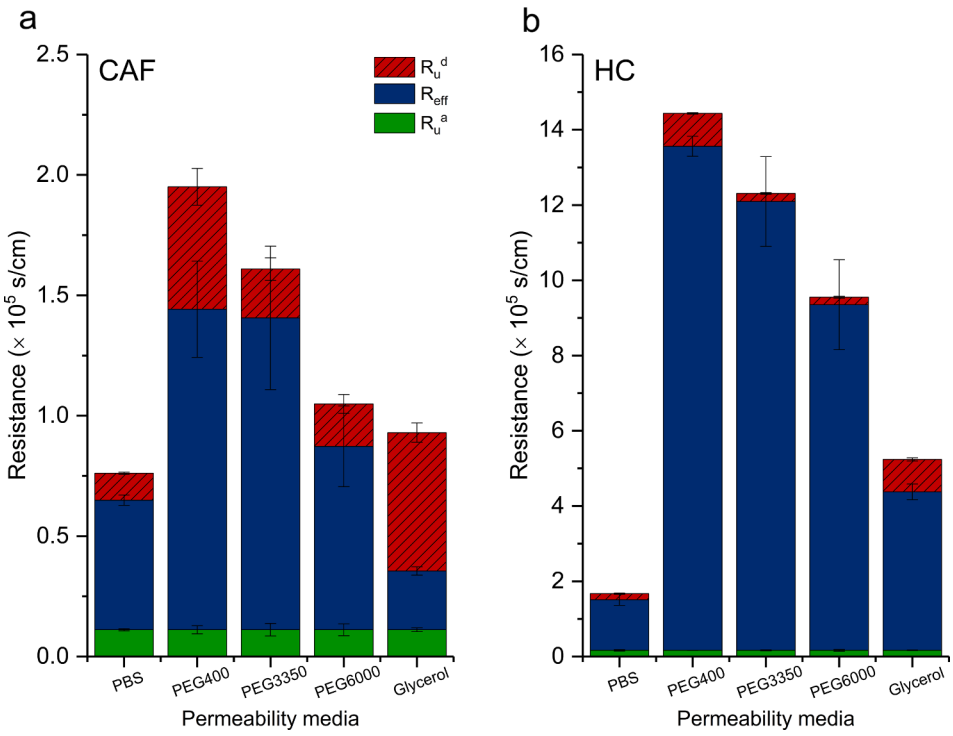

Fig. 7. Resistance to permeability through unstirred water layers on the donor (R_u^d) and acceptor side (R_u^a) and through biomimetic Permeapad® membrane (R_{eff}) for: a) caffeine (CAF) and b) hydrocortisone (HC). Total column height shows the total resistance to permeability (R_{app}) as defined by Eq. (2). The concentrations of each viscosity-enhancing agent were as follows: 40, 25, 15 and 60% for PEG 400, 3350, 6000 and glycerol, respectively. Error bars show SD (n = 3).

(i.e. lower resistivity) in comparison to HC is expected and well in agreement with previous findings (Di Cagno et al., 2015; Jacobsen et al., 2020). The lowest R_{app} was measured in PBS solutions, whereas the highest resistance was measured in PEG 400, for both compounds.

Further, since the permeation experiments were conducted with donor media of comparable viscosities, it appears that PEG's effect on permeation decreases with increasing polymer chain length, for both APIs. However, the comparable viscosities were achieved at different PEG concentrations, which indicates that the presence of more ethylene glycol ($-O-CH_2-CH_2$; EG) units increases the total number of interactions between PEG and API to such extend that this might have a greater influence on the reduction in permeability rate than the solution viscosity. A different explanation of the observed changes could come from the discrepancy between measured viscosity in the bulk solution and the microviscosity, actually encountered by the drugs. The latter would be an interesting area for further studies of UWLs, as the existence of such rheological discrepancies for the *in vivo* UWL of mucus has already been acknowledged (review by Lai et al., 2009).

Focusing on the role of UWL in the permeation process, it is evident that for HC, the major resistance to permeation is the barrier itself (i.e. R_{eff}) independent of the nature of the donor solution, whereas for CAF, the UWL ($R_u^d + R_u^a$) constitutes a significant barrier to permeation, accounting for between 30 (PBS) to 74% (glycerol) of R_{app}. This finding suggests that for hydrophilic moieties, the diffusion through UWL might be the limiting (i.e. rate-determining) step in the permeation process. This is in agreement with the observation of Dahan et al. (2010) that UWL does not limit P_{app} of lipophilic drug progesterone at higher stirring rates (>50 rpm) and the earlier reported apparently thicker UWL met by compounds with larger D, compared to ones with smaller D (Pohl et al., 1998).

In our experiments, in the presence of high glycerol concentrations, CAF diffused slower through the UWLs than through the biomimetic membrane (i.e. $(R_u^d + R_u^a) > R_{eff}$). Due to the relatively hydrophilic nature of both CAF and glycerol, it can be assumed that the interactions between their molecules slow the diffusion of CAF. In the case of HC, $(R_u^d + R_u^a) \ll R_{eff}$ in all media and $(R_u^d + R_u^a)$ in glycerol is still one of the highest of all experiments, comparable only to that of the PEG 400 experiments (1.74 vs 1.72 $\times$ 10^5 s/cm, respectively). This further supports the hypothesis that both glycerol and PEG 400 interact with the hydration shell of the drug molecules and thus alter their diffusivity. Additionally, glycerol is a relatively small molecule that at high concentrations might interact with the biomimetic barrier, making the barrier more "leaky" and influencing drug permeability (i.e. decreasing R_{eff} for all drugs).

3.3.1. Correlation between R_{eff} and $K_{o/w}$

Upon transitioning from the aqueous environment of the donor compartment into the relatively more lipophilic Permeapad® membrane, the behaviour of the molecules can be compared to their partitioning between octanol and water/aqueous phase ($K_{o/w}$). The results of the present study show (Fig. 8) that the distribution coefficients ($K_{o/w}$) of CAF are much lower than HC for all media investigated. Moreover, for HC, $K_{o/w}$ significantly decreases in the presence of hydrophilic polymers, such as PEG, and the reduction can be ranked as follows: PEG 6000 < PEG 3350 < PEG 400. Both glycerol and PEGs act as cosolvents upon addition to the donor solution, altering the nature of the solution by reducing the tension between the aqueous PBS and the relatively more hydrophobic drug molecules. The result is a reduction in drug partitioning to the lipophilic octanol phase and, thus, reduction in $K_{o/w}$.

There was no good correlation between $K_{o/w}$ and R_{eff} values for CAF (Fig. 8, red box) whereas, interestingly, there was an excellent correlation ($R = -0.95$) between R_{eff} and $K_{o/w}$ (excluding glycerol) for HC (Fig. 8, red dashed line). It is noteworthy that octanol/water systems for investigating partitioning generally fail to interpret measured permeability (Magalhães et al., 2010). Studies have shown that membrane-like systems (based on the partitioning between a phospholipid suspension and an aqueous phase) can account for the interactions between drug and polar head groups. Such methods could therefore be better suited for predicting drug permeability and overall absorption kinetics (Carvalho et al., 2020; Lucio et al., 2010). However, in this case, the observed reduction in partitioning translates quite well to the higher resistance to permeation (R_{app}).

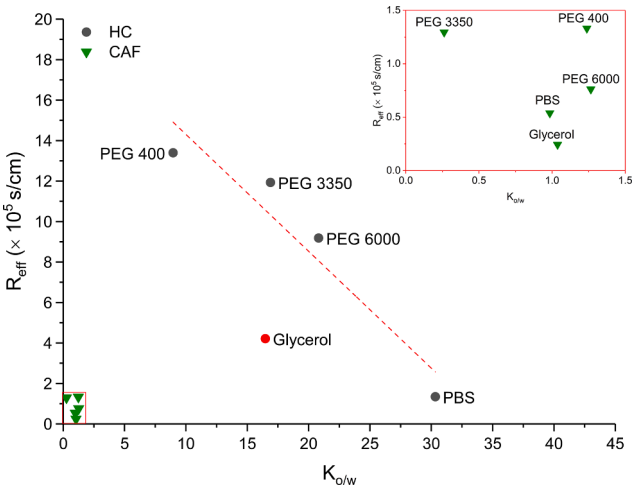

Fig. 8. Relationship between distribution coefficient octanol/aqueous phase ($K_{o/w}$) for CAF (▼) and HC (●) in each of the following aqueous phases: PBS or PBS mixed with PEG 400 (40%), PEG 3350 (25%), PEG 6000 (15%) or glycerol (60%). No linear correlation was observed for the CAF data (inset in upper right corner) but a good one for HC (dashed red line; $R = -0.95$), when excluding glycerol (●).

Further, the fact that glycerol is an outlier in this correlation is not surprising, as glycerol is a rather small molecule capable of permeating through the Permeapad® barrier and acting as a permeation enhancer (Björklund et al., 2013). On the other hand, partitioning seems to have little/no influence on CAF's resistance to permeation. This observation ultimately confirms the validity of our investigations and suggests that the permeation mechanistic of HC and CAF are very different. In fact, for HC the rate-limiting step in the permeation process is its partitioning between the lipophilic membrane and the hydrophilic donor solution whereas, for CAF, the kinetics of permeation are primarily influenced by its diffusion through the UWL and water environments, in general. Further research on a larger set of compounds should be conducted in order to generalize our findings.

4. Conclusions

In this work, we proved that it is possible to discriminate between the role of the UWL and the barrier itself in *in vitro* permeation studies, by direct measurement of passive diffusion of API in UWL-like media. Hydrophilic viscosity-enhancing agents highly influenced the passive diffusion of CAF and HC through the UWL. This phenomenon could be explained only partially by the increase in bulk media viscosity. Molecular-space specific intermolecular drug-polymer interactions and/or microviscosity presumably also play a role. At comparable viscosities, the diffusion of both drugs was more strongly affected by glycerol and PEG 400 than larger PEGs (3350 and 6000). For the hydrophilic drug CAF, the UWL posed a major barrier to drug permeation, whereas, for the lipophilic drug HC, the partitioning aqueous media-barrier was the limiting step to permeation. In other words, the kinetics of permeation indicate that CAF's permeation is mostly a diffusion-driven process, whereas for HC it is mostly a partition-driven one. Glycerol had a huge negative impact on passive diffusion for both drug, without significantly affecting drug permeability. This effect can be explained appropriately by a compensation effect, as glycerol seems to interact with the barrier directly. This approach and findings might have a significant impact on

the design of future formulations, as they could help to enlighten unresolved mechanistic issues of the drug absorption phenomenon.

CRediT authorship contribution statement

Martina M. Tzanova: Methodology, Validation, Formal analysis, Investigation, Writing – original draft, Writing – review & editing, Visualization. **Elizabeta Randelov:** Methodology, Formal analysis, Investigation. **Paul C. Stein:** Methodology, Software, Writing – original draft. **Marianne Hiorth:** Methodology, Supervision, Writing – original draft. **Massimiliano Pio di Cagno:** Conceptualization, Methodology, Resources, Writing – original draft, Writing – review & editing, Supervision, Project administration.

Declaration of Competing Interest

The authors declare the following financial interests/personal relationships which may be considered as potential competing interests: [Massimiliano Pio di Cagno reports equipment, drugs, or supplies was provided by Innome GmbH. Masismiliano Pio di Cagno reports a relationship with Innome GmbH that includes: consulting or advisory. Massimiliano Pio di Cagno has patent #EP3221687B1 licensed to Innome GmbH.].

Acknowledgements

The authors would like to thank Tove Larsen and Ivar Grove for the invaluable technical support and Innome GmbH for providing the Permeapad® plates utilized in this work.

Funding

This research did not receive any specific grant from funding agencies in the public, commercial, or not-for-profit sector.

Appendix A. Supplementary material

Supplementary data to this article can be found online at https://doi.org/10.1016/j.ijpharm.2021.121116.

References

Artursson, P., Karlsson, J., 1991. Correlation between oral drug absorption in humans and apparent drug permeability coefficients in human intestinal epithelial (Caco-2) cells. Biochem. Biophys. Res. Commun. 175 (3), 880–885.

Avdeef, A., Nielsen, P.E., Tsinman, O., 2004. PAMPA—a drug absorption in vitro model: 11. Matching the in vivo unstirred water layer thickness by individual-well stirring in microtitre plates. Eur. J. Pharm. Sci. 22, 365–374.

Avdeef, A., Strafford, M., Block, E., Balogh, M.P., Chambliss, W., Khan, I., 2001. Drug absorption in vitro model: filter-immobilized artificial membranes: 2. Studies of the permeability properties of lactones in Piper methysticum Forst. Eur. J. Pharm. Sci. 14 (4), 271–280.

Barrie, J.A., Levine, J.D., Michaels, A.S., Wong, P., 1963. Diffusion and solution of gases in composite rubber membranes. Trans. Faraday Soc. 59, 869–878.

Berben, P., Bauer-Brandl, A., Brandl, M., Faller, B., Flaten, G.E., Jacobsen, A.-C., Brouwers, J., Augustijns, P., 2018. Drug permeability profiling using cell-free permeation tools: Overview and applications. Eur. J. Pharm. Sci. 119, 219–233.

Bhanot, C., Trivedi, S., Gupta, A., Pandey, S., Pandey, S., 2012. Dynamic viscosity versus probe-reported microviscosity of aqueous mixtures of poly(ethylene glycol). J. Chem. Thermodyn. 45 (1), 137–144.

Björklund, S., Engblom, J., Thuresson, K., Sparr, E., 2013. Glycerol and urea can be used to increase skin permeability in reduced hydration conditions. Eur. J. Pharm. Sci. 50 (5), 638–645.

Blokhina, S.V., Volkova, T.V., Golubev, V.A., Perlovich, G.L., 2017. Understanding of Relationship between Phospholipid Membrane Permeability and Self-Diffusion Coefficients of Some Drugs and Biologically Active Compounds in Model Solvents. Mol. Pharm. 14 (10), 3381–3390.

Brewster, M.E., Noppe, M., Peeters, J., Loftsson, T., 2007. Effect of the unstirred water layer on permeability enhancement by hydrophilic cyclodextrins. Int. J. Pharm. 342 (1-2), 250–253.

Carvalho, A.M., Fernandes, E., Gonçalves, H., Giner-Casares, J.J., Bernstorff, S., Nieder, J.B., Real Oliveira, M.E.C.D., Lúcio, M., 2020. Prediction of paclitaxel pharmacokinetic based on in vitro studies: Interaction with membrane models and human serum albumin. Int. J. Pharm. 580, 119222. https://doi.org/10.1016/j.ijpharm.2020.119222.

Dahan, A., Miller, J.M., Hoffman, A., Amidon, G.E., Amidon, G.L., 2010. The Solubility-Permeability Interplay in Using Cyclodextrins as Pharmaceutical Solubilizers: Mechanistic Modeling and Application to Progesterone. J. Pharm. Sci. 99 (6), 2739–2749.

di Cagno, M., Bibi, H.A., Bauer-Brandl, A., 2015. New biomimetic barrier Permeapad™ for efficient investigation of passive permeability of drugs. Eur. J. Pharm. Sci. 73, 29–34.

di Cagno, M.P., Clarelli, F., Våbenø, J., Lesley, C., Rahman, S.D., Cauzzo, J., Franceschinis, E., Realdon, N., Stein, P.C., 2018. Experimental Determination of Drug Diffusion Coefficients in Unstirred Aqueous Environments by Temporally Resolved Concentration Measurements. Mol. Pharm. 15 (4), 1488–1494.

di Cagno, M.P., Stein, P.C., 2019. Studying the effect of solubilizing agents on drug diffusion through the unstirred water layer (UWL) by localized spectroscopy. Eur. J. Pharm. Biopharm. 139, 205–212.

Falavigna, M., Stein, P., Flaten, G., di Cagno, M., 2020. Impact of Mucin on Drug Diffusion: Development of a Straightforward in Vitro Method for the Determination of Drug Diffusivity in the Presence of Mucin. Pharmaceutics 12 (2), 168. https://doi.org/10.3390/pharmaceutics12020168.

Flynn, G.L., Yalkowsky, S.H., Roseman, T.J., 1974. Mass transport Phenomena and Models: Theoretical Concepts. J. Pharm. Sci 63 (4), 479–510.

Grassi, M., Colombo, I., 1999. Mathematical modelling of drug permeation through a swollen membrane. J. Control Release 59 (3), 343–359.

Hirai, M., Ajito, S., Sugiyama, M., Iwase, H., Takata, S.-I., Shimizu, N., Igarashi, N., Martel, A., Porcar, L., 2018. Direct Evidence for the Effect of Glycerol on Protein Hydration and Thermal Structural Transition (vol 115, pg 313, 2018). Biophys. J. 115 (4), 748.

Hou, S., Ziebacz, N., Kalwarczyk, T., Kaminski, T.S., Wieczorek, S.A., Holyst, R., 2011. Influence of nano-viscosity and depletion interactions on cleavage of DNA by enzymes in glycerol and poly(ethylene glycol) solutions: qualitative analysis. Soft Matter 7 (7), 3092–3099.

Jacobsen, A.-C., Nielsen, S., Brandl, M., Bauer-Brandl, A., 2020. Drug Permeability Profiling Using the Novel Permeapad® 96-Well Plate. Pharm. Res. 37, 93.

Karlsson, J., Artursson, P., 1991. A method for the determination of cellular permeability coefficients and aqueous boundary layer thickness in monolayers of intestinal epithelial (Caco-2) cells grown in permeable filter chambers. Int. J. Pharm. 71 (1-2), 55–64.

Korjamo, T., Heikkinen, A.T., Mönkkönen, J., 2009. Analysis of Unstirred Water Layer in In Vitro Permeability Experiments. J. Pharm. Sci. 98 (12), 4469–4479.

Kwatra, D., Boddu, S.H.S., Mitra, A.K., 2011. In: Oral Bioavailability: Basic Principles, Advanced Concepts, and Applications. John Wiley & Sons, Inc., Hoboken, NJ, USA, pp. 443–459. https://doi.org/10.1002/9781118067598.ch28.

Lai, S.K., Wang, Y.-Y., Wirtz, D., Hanes, J., 2009. Micro- and macrorheology of mucus. Adv. Drug Deliv. Rev. 61 (2), 86–100.

Lennernaäs, H., 1998. Human Intestinal Permeability. J. Pharm. Sci. 87 (4), 403–410.

Loftsson, T., Konrádsdóttir, F., Másson, M., 2006. Development and evaluation of an artificial membrane for determination of drug availability. Int. J. Pharm. 326 (1-2), 60–68.

Lucio, M., Lima, J.L.F.C., Reis, S., 2010. Drug-Membrane Interactions: Significance for Medicinal Chemistry. Curr. Med. Chem. 17, 1795–1809.

Magalhães, L.M., Nunes, C., Lúcio, M., Segundo, M.A., Reis, S., Lima, J.L.F.C., 2010. High-throughput microplate assay for the determination of drug partition coefficients. Nat. Protoc. 5 (11), 1823–1830.

Pohl, P., Saparov, S.M., Antonenko, Y.N., 1998. The Size of the Unstirred Layer as a Function of the Solute Diffusion Coefficient. Biophys. J. 75 (3), 1403–1409.

Price, W.E., 1989. Tracer caffeine diffusion in aqueous solutions at 298 K. The effect of caffeine self-association. J Chem Soc, Faraday Transactions 1: Physical Chemistry in Condensed Phases 85 (2), 415. https://doi.org/10.1039/f19898500415.

Zhong, H., Chan, G., Hu, Y., Hu, H., Ouyang, D., 2018. A Comprehensive Map of FDA-Approved Pharmaceutical Products. Pharmaceutics 10 (4), 263. https://doi.org/10.3390/pharmaceutics10040263.